

# Toughening mechanisms of modified unsaturated polyester with novel liquid polyurethane rubber

D. S. KIM, K. CHO, J. H. AN, C. E. PARK

*Organic Materials Division, Research Institute of Industrial Science and Technology, and Department of Chemical Engineering, Pohang University of Science and Technology, P.O. Box 125, Pohang 790-600, Korea*

Unsaturated polyester (UPE) has been toughened by incorporating novel liquid polyurethane (PU) rubber. PU rubber was synthesized using toluene di-isocyanate and polyols such as poly(propylene glycol) and poly(tetramethylene ether) glycol, whose molecular weights vary from 650 to 4000. Particle size was varied from 0.1 to 3  $\mu\text{m}$  by changing the polyol and the molecular weight of PU rubber, and the effects of particle size on the fracture toughness of PU rubber-modified UPE were investigated. Hydroxyl terminated PU rubber (HTPU) and isocyanate terminated PU rubber (ITPU) were used to study the effects of rubber–matrix adhesion. The toughening mechanisms observed by scanning electron microscope are debonding between rubber and matrix in HTPU-modified UPE, and cavitation in the rubber particle in ITPU-modified UPE. However, shear bands were not observed as UPE is a highly cross-linked thermoset with very short chain length between the cross-links. A 1.9-times increase in fracture toughness of UPE was achieved with the formation of cavitated particles. In order to measure the process zone size at the crack tip, the thin sections of tested double-notched four-point bending specimens were examined by optical microscope.

## 1. Introduction

Rubber toughening of thermosets has been studied since Sultan and co-workers [1] improved the fracture toughness of an epoxy by incorporating rubber. Many researchers have investigated the toughening mechanisms of rubber-modified epoxies. It is now well recognized that crazing, which is the major toughening mechanism of thermoplastics, cannot be the toughening mechanism of thermosets because the cross-linked structures suppress the formation of crazing [2]. Recently, Huang & Kinloch [3, 4] developed a quantitative mathematical model demonstrating three different toughening mechanisms of rubber-modified epoxies, i.e. shear bands which occur between the rubber particles [5, 6], plastic void growth which is initiated by cavitation or debonding of the rubber particles [7, 8], and rubber bridging [9]. They also predicted that the contribution of plastic void growth increases sharply with rising temperature, and the rubber bridging mechanism can play an important role when the ability of the matrix to undergo plastic deformation is suppressed.

Pearson & Yee [10] showed that toughness enhancement is achieved by two energy dissipating mechanisms at the crack tip for rubber-modified epoxies: firstly, internal cavitation of the rubber particles, and subsequently shear band formation in the epoxy matrix, which is the major energy dissipating mechanism. The quantity of shear bands is dependent on

the ductility of matrix: shear band formation decreases with increasing cross-link density of matrix and shear band was not observed with rubber-modified highly cross-linked epoxy (e.g. diglycidyl ether of bisphenol A (DGEBA) epoxy hardened with diaminodiphenyl sulfone (DDS) instead of piperidine).

It is well known that the particle size of rubber, adhesion strength between rubber particle and matrix, and properties of rubber particles are important parameters affecting the fracture toughness and the toughening mechanism of rubber-modified polymers. Pearson & Yee [11] studied the rubber particle size effects – smaller particles provide a significant increase in toughness by cavitation-induced shear bands, whereas large particles provide only a modest increase in fracture toughness by a particle bridging/crack deflection mechanism. They also showed that large particles cannot be cavitated because they lie outside the plastic zone proposed by Irwin [12] where the large hydrostatic stress exists. Although rubber–matrix adhesion is important for good stress transfer ability and properties of rubber particles determine the cavitation resistance of rubber, systematic studies on the above parameters have not been carried out with thermosets. Furthermore, as these three parameters are closely related and cannot be adjusted independently, it is difficult to analyse the effects of individual parameters on the fracture toughness of thermosets.

Unsaturated polyester (UPE) is a highly cross-linked resin, whose cross-linked density is even higher than DDS-hardened DGEBA epoxy. Rubber toughening of UPE with reactive liquid rubber based on a butadiene-acrylonitrile copolymer has been studied [13–16], but little work has been reported describing toughening mechanisms of UPE. In this study, UPE has been toughened with novel liquid polyurethane rubber made in our laboratory, and toughening mechanisms of PU-rubber-modified UPE have been investigated by varying the rubber–matrix adhesion and the particle size from 0.1–3  $\mu\text{m}$ . As the volume fraction and the properties of the rubber particles are also varied with changes of particle size, these effects on rubber toughening of UPE are also examined.

## 2. Experimental procedure

### 2.1. Materials

The terephthalic unsaturated polyester (Aekyung Chemical Co.) with 35 wt % styrene content was cured using 1.75 p.h.r. (parts per hundred resins) methylethyl ketone peroxide as a curing agent and 0.42 p.h.r. cobalt-octate (metal content 12%) as an accelerator. Chemicals used for polyurethane rubber were toluene diisocyanate (80:20 mixture of 2,4- and 2,6-toluene diisocyanate, Aldrich Chemical Co.), poly (tetramethylene ether) glycol of molecular weights from 650 to 2000 (Scientific Polymer Products, Inc.), polypropylene glycol of molecular weights from 750 to 4000 (Korea Polyol), and 1,4-butanediol (Polyscience).

### 2.2. Synthesis of liquid polyurethane rubber

Liquid polyurethane rubber was synthesized by a two-step procedure. In the first step, TDI reacted with polyols in the molar ratio of 2:1 to form an isocyanate terminated prepolymer (TDI–polyol–TDI). In the second step, the prepolymer reacted with 1,4-butanediol (BD) as a chain extender to form liquid polyurethane rubber. In order to control the compatibility of rubber with UPE, two polyols with different polarity, PPG and PTMG were used, and molecular weights of polyols varied from 650 to 4000. In order to study the adhesion effect on toughening, isocyanate or hydroxyl terminated polyurethane rubbers were synthesized by varying the molar ratio of prepolymer and BD as 2:1

or 2:3, respectively. The details of reaction procedures have been published elsewhere [17].

Table I shows the molecular weights of PU rubbers obtained by theoretical calculation, titration and gel permeation chromatography. Molecular weights of hydroxyl terminated PU rubbers were determined by titrating the hydroxyl group with acetic anhydride, and those of isocyanate terminated PU rubbers were determined by titrating the isocyanate group with *n*-butylamine. The measured molecular weights by gel permeation chromatography with three  $\mu$ -styragel columns (10.0, 50.0 and 100.0 nm) using tetrahydrofuran as a solvent were always higher than those by theoretical calculation or titration, as polystyrene was used as a standard for gel permeation chromatography.

### 2.3. Curing of UPE

After mixing 10 p.h.r. synthesized liquid PU rubber and UPE at 60 °C, the mixture was poured into two Teflon-coated aluminium moulds with a silicone rubber spacer measuring 300  $\times$  300  $\times$  6 mm and was cured at 60 °C for 5 h.

### 2.4. Mechanical properties

Fracture toughness,  $K_{IC}$ , was measured by a notched three-point bending test according to ASTM E-399. A sharp crack was introduced by carefully tapping a fresh razor blade into the base of the saw cut. Fracture toughness,  $K_{IC}$ , was calculated as described elsewhere [17].

Flexural properties such as flexural strength, flexural modulus and strain at break were measured by the three-point bending test according to ASTM D-790. Before mechanical testing, specimens were post-cured at 80 °C for 1 h to release the residual stress. Eight specimens per test were examined for all mechanical properties studies. Further details of both tests are described elsewhere [17].

### 2.5. Microscopy

After the fracture test, the fracture surfaces were examined by scanning electron microscope (SEM). The particle size and volume fraction of rubber particles were examined using an image analyser, with six micrographs for each sample.

TABLE I Molecular weights of synthesized polyurethane rubber

Polyol	Hydroxyl-terminated PU			Isocyanate-terminated PU		
	Theoretical	Titration	GPC	Theoretical	Titration	GPC
PTMG 650	2267	1920	3610	2087	2600	5240
PTMG 1000	2967	3030	5820	2787	3430	5700
PTMG 2000	4967	4220	8850	4787	6940	14570
PPG 750	2467	2340	3350	2287	3840	5300
PPG 1000	2967	2620	3530	2787	4000	6950
PPG 2000	4967	4220	5780	4787	7240	11300
PPG 4000	8967	5600	–	8787	9800	–

The mature process zone at the crack tip of the double-notched four-point bending (DN-4PB) specimen was examined by transmitted optical microscope [11, 18]. Fig. 1 shows the geometry of the DN-4PB specimen. There are two nearly identical sharp cracks cut into the same edge of the specimen with a fresh razor blade. The ratio between the crack spacing and

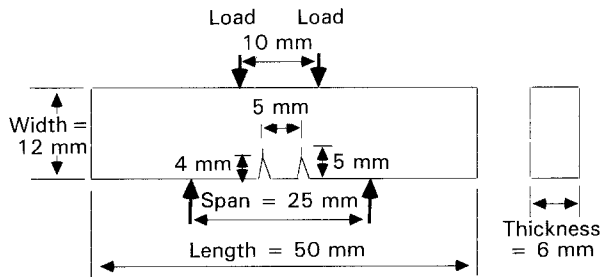


Figure 1 Geometry of the double-notched four-point bending specimen.

the crack length must be greater than 0.75 in order to eliminate the interaction between the two cracks [19, 20]. The specimens were tested at the crosshead speed of  $0.5 \text{ mm min}^{-1}$ . Loading the specimen, one crack will propagate but the other will not because the cracks cannot be precisely identical. Therefore the stationary crack has the mature process zone at the crack tip. The thin sections are taken in the mid-plane (plane strain region) near the stationary crack of the fractured DN-4PB specimens, which are normal to the fractured surface and parallel to fracture direction. A petrographic polishing technique was employed to obtain the thin sections of about  $100 \mu\text{m}$  for transmitted optical microscopy [11, 21].

Tensile tests were also carried out in order to find out the shear band formation. ASTM D-638 type I specimens were prepared using a high speed router (Tensilkut). The tensile specimens were tested at the crosshead speed of  $50 \text{ mm min}^{-1}$ . The thin section was taken parallel to the tensile direction and near the

TABLE II Fracture toughness of HTPU-modified UPE

PU rubber*	Molecular weight of rubber†	Particle size ( $\mu\text{m}$ )	Vol. per cent of rubber	Fracture toughness $K_{Ic}$ ( $\text{MN m}^{-3/2}$ )
Neat UPE	—	—	—	$0.49 \pm 0.03$
PTMG 650	1920	$0.94 \pm 0.63$	9	$0.75 \pm 0.05$
PTMG 1000	3030	$1.03 \pm 0.73$	25	$0.74 \pm 0.05$
PTMG 2000	4220	$1.31 \pm 1.28$	32	$0.77 \pm 0.02$
PPG 750	2340	—	—	$0.74 \pm 0.05$
PPG 1000	2620	$0.15 \pm 0.10$	3	$0.75 \pm 0.05$
PPG 2000	4220	$1.33 \pm 1.56$	31	$0.74 \pm 0.06$
PPG 4000	5600	$2.93 \pm 3.42$	30	$0.68 \pm 0.07$

\* Rubber content: 10 p.h.r.

† Molecular weight of PU rubber measured by titrating end groups.

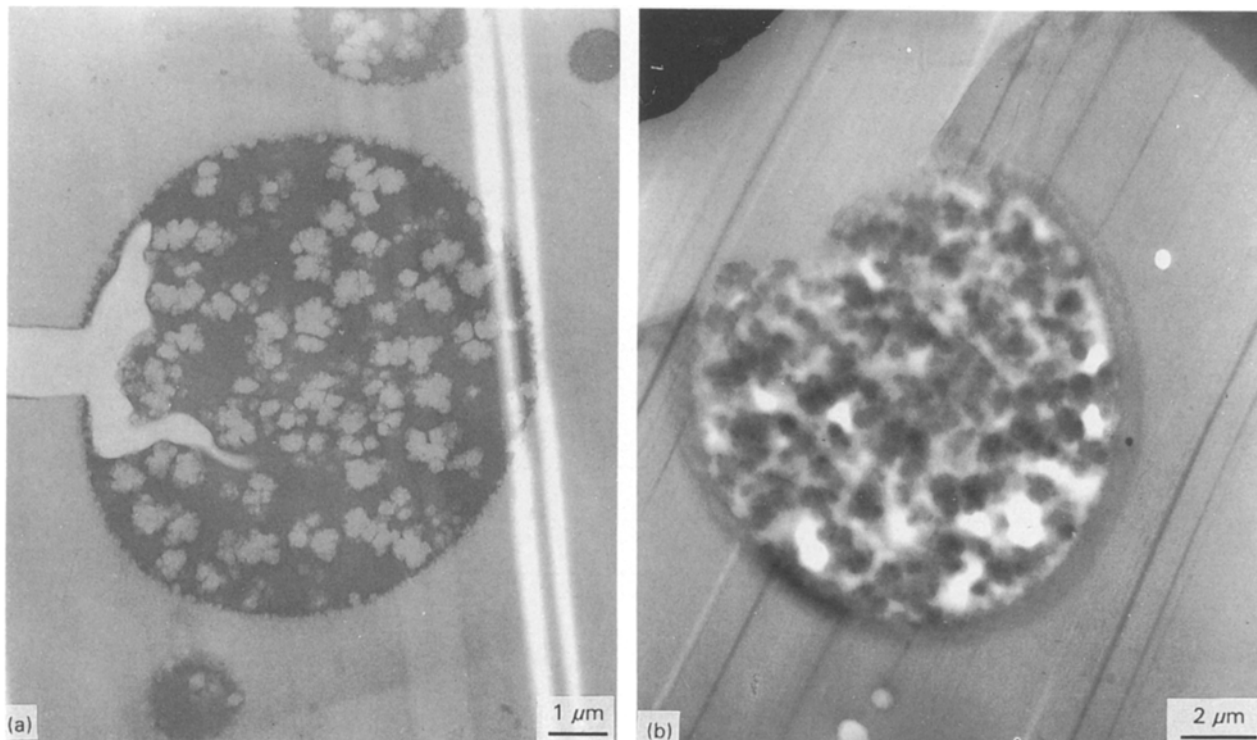


Figure 2 TEM micrographs of 10 p.h.r. ITPU-modified UPE based on (a) PTMG 1000, (b) PPG 1000.

broken region of the tensile specimen by the same method as used for DN-4PB. These samples were examined using a Carl Zeiss Axioplan optical microscope under bright-field and crossed polarization.

### 2.6. Dynamic mechanical thermal analysis

The glass transition temperatures ( $T_g$ ) of rubber and matrix were determined using dynamic mechanical thermal analyser (DMTA, Polymer Laboratory). The dimensions of the specimen were 2.5 mm thick, 7 mm wide and 20 mm long. The specimen was tested in a single cantilever mode and scanned at a frequency of 1 Hz from  $-80$  to  $250^\circ\text{C}$  with a heating rate of  $3^\circ\text{C min}^{-1}$ . The temperature at which the  $\tan \delta$  peak appeared was quoted as the  $T_g$ .

## 3. Results and discussion

### 3.1. Hydroxyl terminated polyurethane rubber (HTPU)-modified UPE

Table II shows the fracture toughness of HTPU-modified UPE. As the molecular weight of PU rubber increases, the particle size and volume fraction of rubber particles also increase. In PPG 750-based HTPU-modified UPE, the rubber particles are too small to be observed by SEM (see Fig. 4a below).

The volume fraction of rubber varies from 3 to 32%, depending on the type of rubber and molecular weight, even though the incorporated rubber content is fixed at 10 p.h.r. The 10 p.h.r. rubber content corresponds to 9 vol% of rubber, assuming the densities of matrix and rubber are equal to 1 [22]. With PPG-based low-molecular-weight PU rubber, less than 9 vol% of rubber particles is obtained, indicating that part of the rubber dissolves in the UPE matrix. On the other hand, with higher molecular weight of PU rubber, more than 9 vol% of rubber particles is obtained, as UPE matrix is incorporated into rubber particles. Fig. 2 shows transmission electron micrographs of PTMG 1000- and PPG 1000-based ITPU-modified UPE, which were exposed to  $\text{OsO}_4$  vapour for 48 h in order to stain PU rubber. UPE inclusions in the PU rubber particle are clearly shown as white domains for PTMG 1000-based PU rubber-modified UPE. A different morphology is shown for PPG 1000-based PU rubber-modified UPE, due to better compatibility of PPG-based PU rubber with UPE.

The fracture toughness of HTUP-modified UPE is increased up to 1.5 times that of the control sample, except PPG 4000-based HTPU-modified UPE, and independent of the molecular weight of HTPU.

Figs 3 and 4 show scanning electron micrographs of fracture surfaces of the stress-whitened region of PTMG- and PPG-based HTPU-modified UPE, respectively. Debonding and extraction of rubber particles from the matrix are clearly shown. As there is no chemical bond between HTPU and the matrix, the adhesion strength between the rubber and matrix seems to be poor and debonding can occur at the interface of rubber and matrix when a load is applied to a specimen. The toughness of HTPU-modified UPE seems to be improved by making voids between

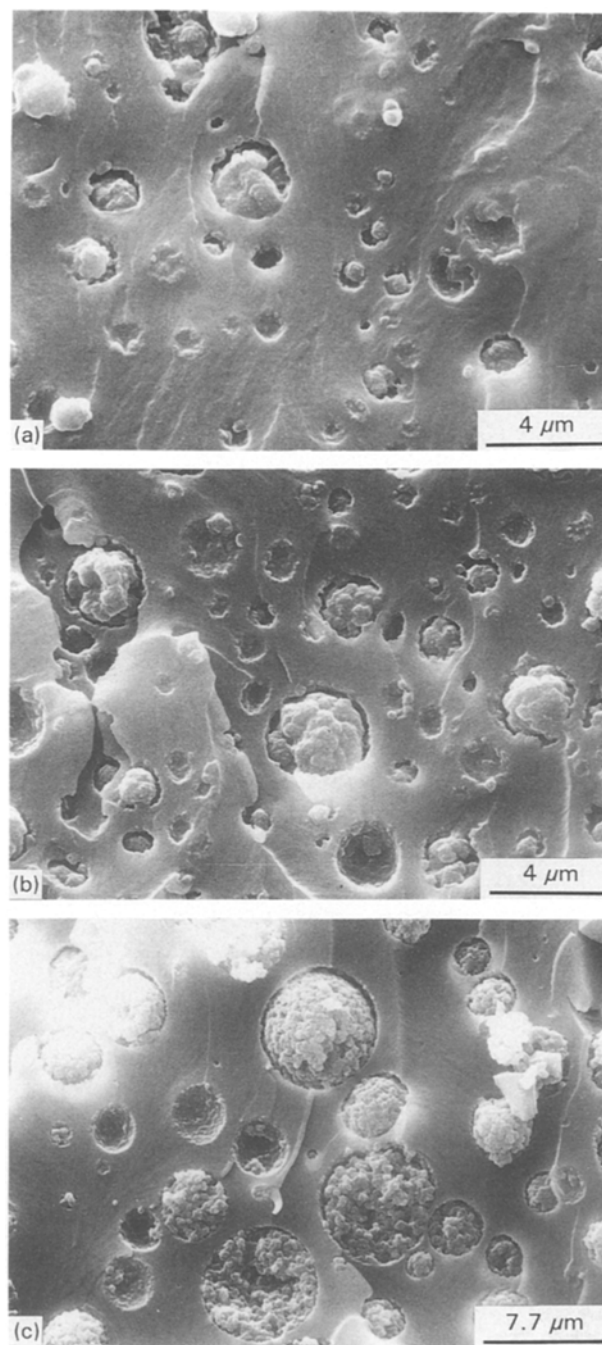


Figure 3 SEM micrographs of fracture surfaces of 10 p.h.r. HTPU-modified UPE based on (a) PTMG 650, (b) PTMG 1000, (c) PTMG 2000.

rubber particles and matrix through debonding. As smaller particles have more interfacial area between rubber particle and matrix, fracture toughness might be improved by reducing the particle size. However, as the rubber particle size decreases, the volume fraction of rubber particle also decreases, because low-molecular-weight PU rubber dissolves in the matrix. Therefore the fracture toughness of HTPU-modified UPE seems to be unaffected by varying the molecular weight of PU rubber, except for PPG 4000.

### 3.2. Isocyanate terminated polyurethane rubber (ITPU)-modified UPE

Table III shows the fracture toughness of ITPU-modified UPE. As the molecular weight of PU rubber

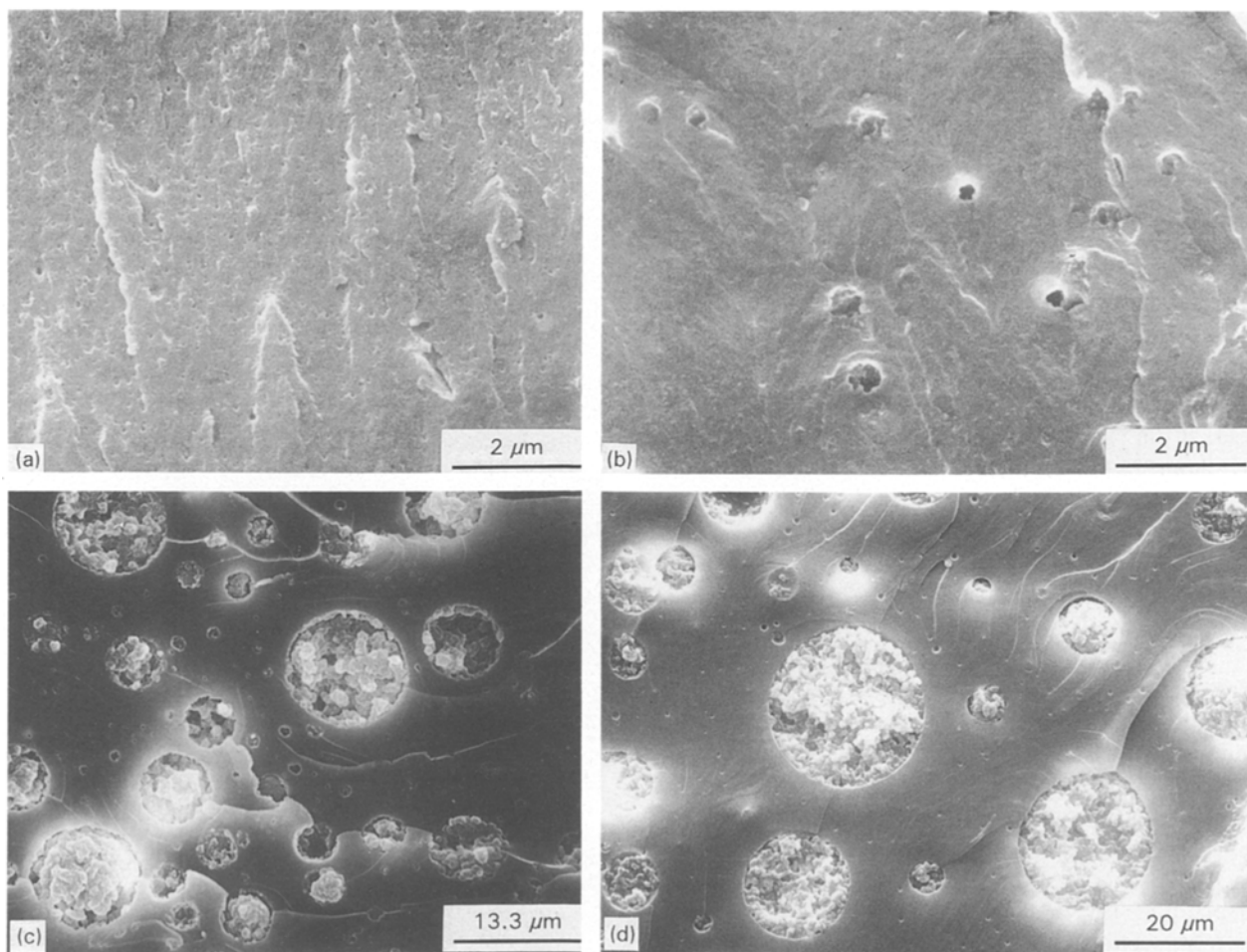


Figure 4 SEM micrographs of fracture surfaces of 10 p.h.r. HTPU-modified UPE based on (a) PPG 750, (b) PPG 1000, (c) PPG 2000, (d) PPG 4000.

TABLE III Fracture toughness of ITPU-modified UPE

PU rubber*	Molecular weight of rubber†	Particle size (μm)	Vol. per cent of rubber	Fracture toughness $K_{IC}$ (MN m <sup>-3/2</sup> )
Neat UPE	—	—	—	0.49 ± 0.03
PTMG 650	2600	—	—	0.69 ± 0.03
PTMG 1000	3430	0.11 ± 0.10	8	0.76 ± 0.05
PTMG 2000	6940	0.67 ± 0.89	25	0.91 ± 0.05
PPG 750	3840	—	—	0.65 ± 0.03
PPG 1000	4000	0.14 ± 0.15	9	0.76 ± 0.06
PPG 2000	7240	1.23 ± 1.46	39	0.89 ± 0.04
PPG 4000	9800	2.85 ± 2.02	30	0.78 ± 0.05

\* Rubber content: 10 p.h.r.

† Molecular weight of PU rubber measured by titrating end groups.

increases, the particle size and volume fraction of rubber particles increase, which is similar to HTPU-modified UPE except for the smaller particle size. As the isocyanate end group of ITPU can react with the hydroxyl or carboxylic acid group of UPE, with the same molecular weight of rubber the particle size of ITPU-modified UPE is reduced due to the lack of mobility of ITPU. And the adhesion strength of the rubber particles with the matrix is expected to be good because of the chemical bonding between rubber particles and matrix.

Figs 5 and 6 show scanning electron micrographs of fracture surfaces of the stress-whitened region of PTMG- and PPG-based ITPU-modified UPE, respectively. In Figs 5 and 6, instead of debonding of rubber particles from the matrix, many cavitations are clearly seen in the rubber particles close to the interface between rubber particles and matrix. The cavitations are clearly shown with higher magnification of the scanning electron micrographs in Fig. 7. In order to find out whether the voids were formed by CO<sub>2</sub> gases generated through the chemical reaction

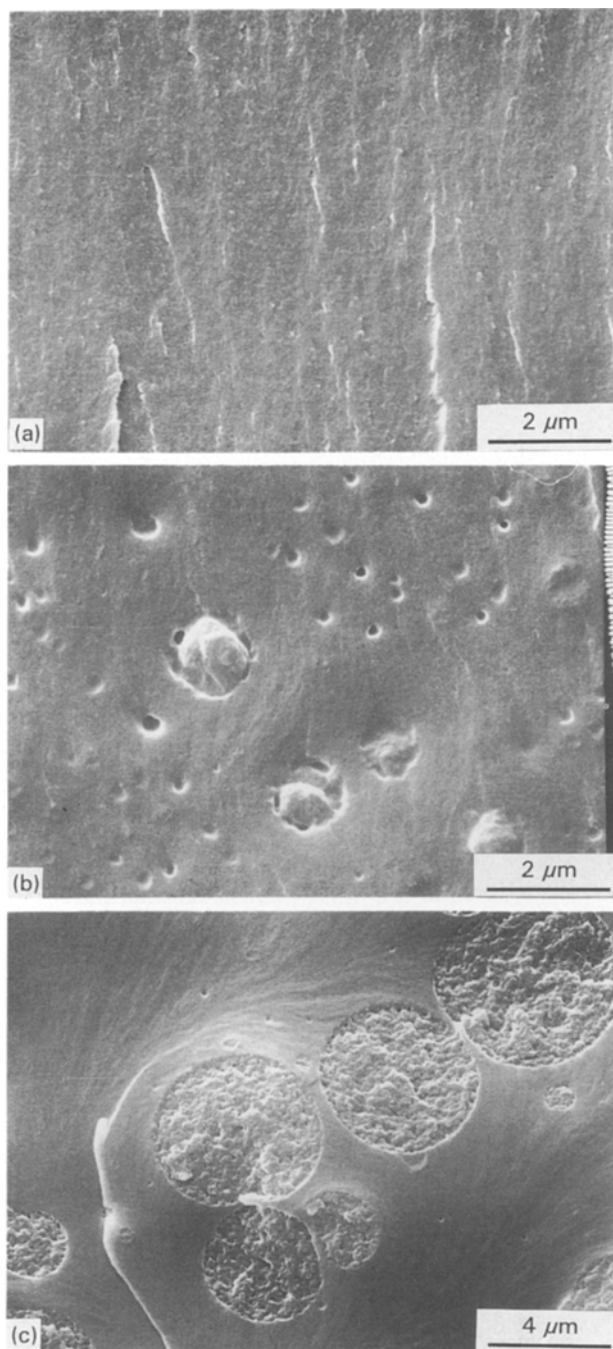


Figure 5 SEM micrographs of fracture surfaces of 10 p.h.r. ITPU-modified UPE based on (a) PTMG 650, (b) PTMG 1000, (c) PTMG 2000.

between isocyanate and carboxylic acid group, a cryogenic fracture test was performed in liquid nitrogen. The void was not formed in the cryogenic fracture test (Fig. 8a) even though many voids are formed in the fracture test at room temperature (Fig. 8b), which confirms that the cavitations are formed by hydrostatic tensile stress near the crack tip.

The fracture toughness of ITPU-modified UPE increases up to 1.9 times that of neat UPE as the molecular weight of ITPU increases, except for PPG 4000-based rubber. It seems that the toughening mechanism of ITPU-modified UPE is the cavitation in the rubber particle. Although a smaller particle size can induce more cavitations in the rubber particle, the

volume fraction of rubber particles is reduced with the system of small particles, because low-molecular-weight rubber dissolves in the matrix. Overall, maximum cavitations seem to be obtained with PTMG 2000- and PPG 2000-based ITPU-modified UPE. By forming chemical bonds between rubber and matrix, the toughening mechanism is changed from the debonding of rubber particles from the matrix to the cavitation in the rubber particles, which seems to improve the fracture toughness from 1.5 to 1.9 times that of neat UPE.

### 3.3. Dynamic mechanical thermal analysis

Dynamic mechanical thermal analysis (DMTA) was employed to study the properties of PU rubber. Generally, there are two glass transition temperatures ( $T_g$ ) in rubber-toughened plastics: one is the  $T_g$  of matrix, the other the  $T_g$  of dispersed rubber particles. The properties of PU rubber can be estimated by the  $T_g$  of dispersed rubber particles.

Fig. 9 shows the DMTA spectrums of unmodified UPE- and PPG 2000-based ITPU-modified UPE. Unmodified UPE shows the  $\tan \delta$  peak at 179 °C, due to UPE main-chain movements and the shoulder near 135 °C caused by the relaxation of polystyrene or UPE-styrene copolymer. PPG 2000-based ITPU-modified UPE shows another transition at -38 °C, due to the relaxation of PU rubber.

Table IV shows the  $T_g$  for UPE matrix and rubber particles, which are obtained from the  $\tan \delta$  peaks of the DMTA spectra.  $T_g$  of PU rubber decreases as the molecular weight of PU rubber increases, as the distance between physical cross-links formed by hard segments increases. As the molecular weight of PU rubber decreases,  $T_g$  of the matrix also shifts to a lower temperature, which proves the better compatibility of rubber and UPE with the lower molecular weight of rubber. This is consistent with the fact that the volume fraction of rubber particles decreases as the molecular weight of rubber decreases. And  $T_g$  of the matrix shifts to a lower temperature with PPG-based PU rubber-modified UPE than those of PTMG-based PU rubber-modified UPE, due to better compatibility of PPG-based PU rubber with UPE. As the particle size, the volume fraction and the properties of rubber change simultaneously by varying the molecular weight of incorporated PU rubber, it is very difficult to discriminate the effects of the particle size, volume fraction, and the properties of rubber experimentally on rubber toughening of highly cross-linked thermosets.

### 3.4. Optical microscopy

Bright-field and cross-polarized light are used to elucidate the nature and the extent of the sub-surface process zone formed ahead of the crack tip. In the bright-field, debonding and cavitation of rubber particles appear almost black as these scatter the light. In the cross-polarized light, shear bands can be seen as shear bands are composed of highly oriented birefringent materials.

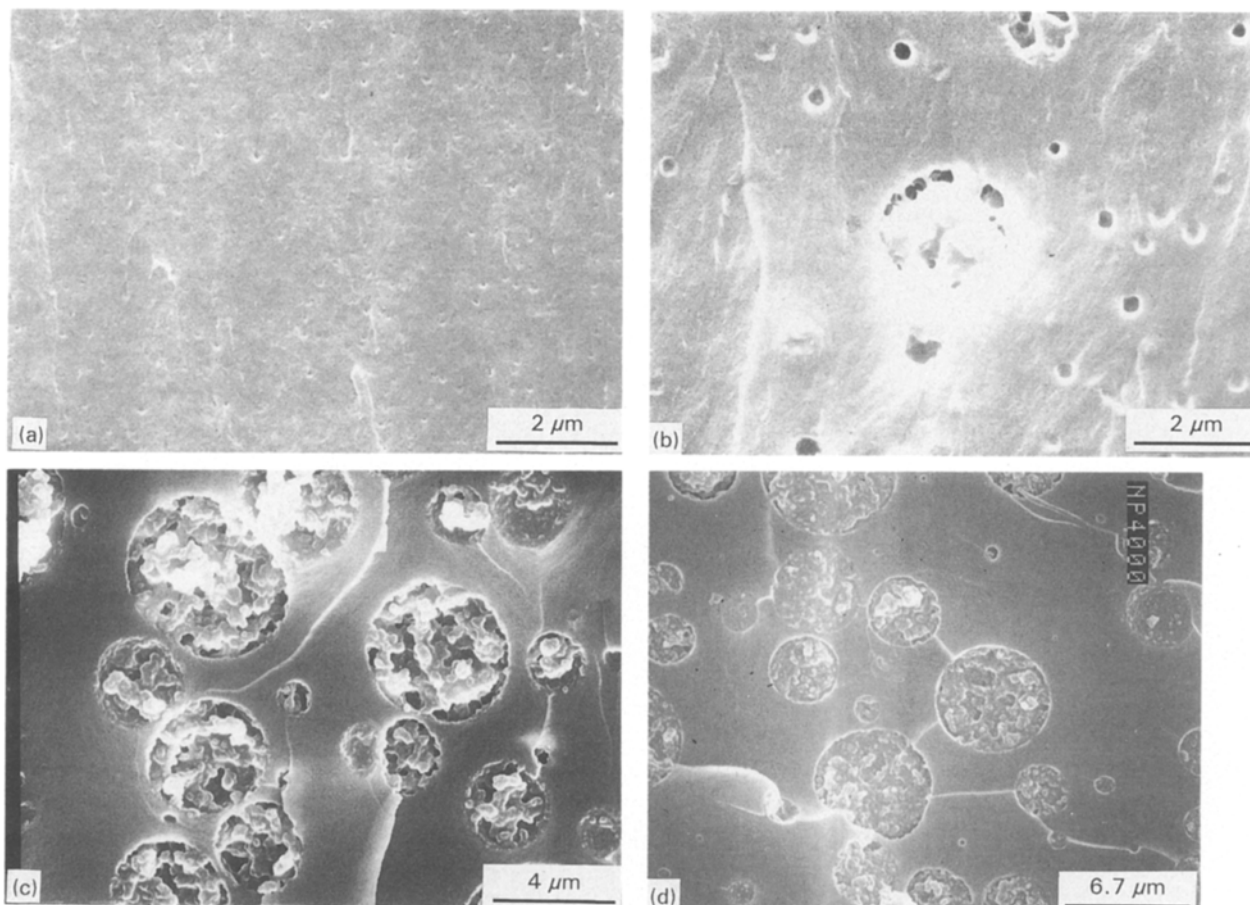


Figure 6 SEM micrographs of fracture surfaces of 10 p.h.r. ITPU-modified UPE based on (a) PPG 750, (b) PPG 1000, (c) PPG 2000, (d) PPG 4000.

TABLE IV  $T_g$  of the PU rubber-modified UPE

	Matrix (°C)	Rubber (°C)
Neat UPE	179	–
PTMG 650-hydroxyl	168	– 5
PTMG 1000-hydroxyl	171	– 25
PTMG 2000-hydroxyl	175	– 50
PTMG 650-isocyanate	175	–
PTMG 1000-isocyanate	176	– 23
PTMG 2000-isocyanate	178	– 55
PPG 750-hydroxyl	167	–
PPG 1000-hydroxyl	167	– 15
PPG 2000-hydroxyl	168	– 38
PPG 4000-hydroxyl	170	– 50
PPG 750-isocyanate	170	–
PPG 1000-isocyanate	175	– 8
PPG 2000-isocyanate	175	– 38
PPG 4000-isocyanate	172	– 50

TABLE V Process zone sizes of PU rubber-modified UPE

PU Rubber*-functional group	Process zone size $r_p$ (μm)
PTMG 650-hydroxyl	50
PTMG 1000-hydroxyl	75
PTMG 2000-hydroxyl	110
PTMG 650-isocyanate	–
PTMG 1000-isocyanate	10
PTMG 2000-isocyanate	345
PPG 750-hydroxyl	10
PPG 1000-hydroxyl	20
PPG 2000-hydroxyl	135
PPG 4000-hydroxyl	–
PPG 750-isocyanate	–
PPG 1000-isocyanate	15
PPG 2000-isocyanate	240
PPG 4000-isocyanate	–

\* Rubber content: 10 p.h.r.

Figs 10 and 11 are optical micrographs of PTMG-based HTPU and ITPU modified-UPE, respectively, showing the circular process zone around the crack tip. The dark process zones originated from light scattering by the empty spaces. The empty spaces are formed by the debonding of rubber particles from the matrix in HTPU-modified UPE, and by the cavitation

of the rubber particles in ITPU-modified UPE. As the molecular weight of rubber increases, the size of the process zone increases; this trend is more pronounced in ITPU-modified UPE. As shown in Fig. 11c, a smaller, darker zone is surrounded by a grey circular zone. The outer grey zone seems to contain slightly cavitated particles and the inner, darker zone contains

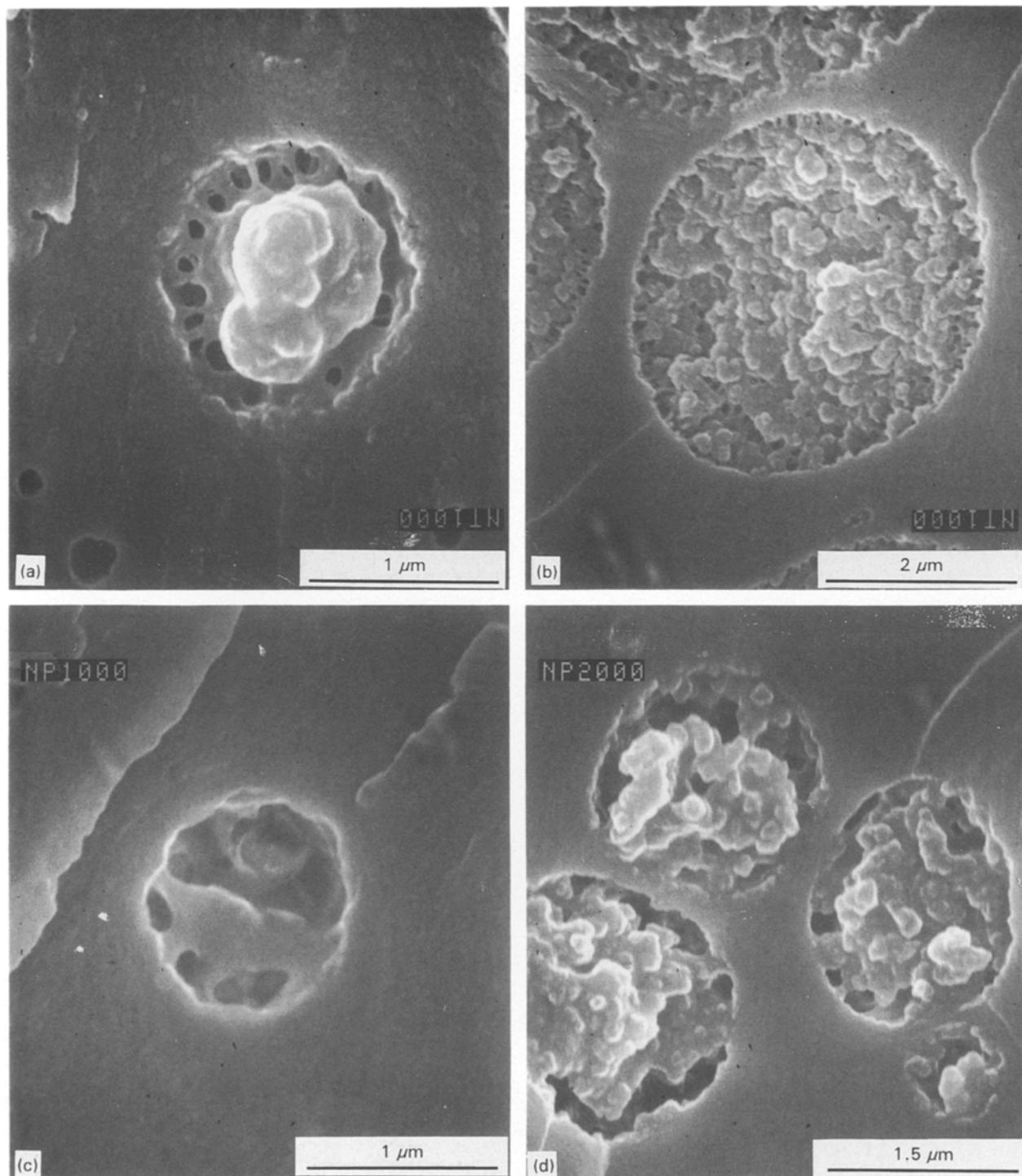


Figure 7 SEM micrographs of fracture surfaces of 10 p.h.r. ITPU-modified UPE based on (a) PTMG 1000, (b) PTMG 2000, (c) PPG 1000, (d) PPG 2000.

highly cavitated particles. This is consistent with the observations by Pearson & Yee [11] on the rubber-modified epoxy. Figs 12 and 13 are optical micrographs of PPG-based HTPU- and ITPU-modified UPE. It is noted that the process zone size becomes much smaller with decreasing molecular weight of PPG-based rubber, while the process zone is not formed in PPG 4000-based HTPU- and ITPU-modified UPE.

Table V shows the process zone sizes of HTPU- and ITPU-modified UPE determined from optical

micrographs. In ITPU-modified UPE, as the process zone size increases, the fracture toughness also increases. However, in HTPU-modified UPE, the fracture toughness is constant even though the process zone size increases. As this moment, it is difficult to explain the experimental results.

Fig. 14 shows optical micrographs of PPG 4000-based HTPU- and ITPU-modified UPE at a higher magnification. The process zone is not shown, but rubber particle bridging is shown. Pearson & Yee [11] proposed an empirical criterion for bridging particles:

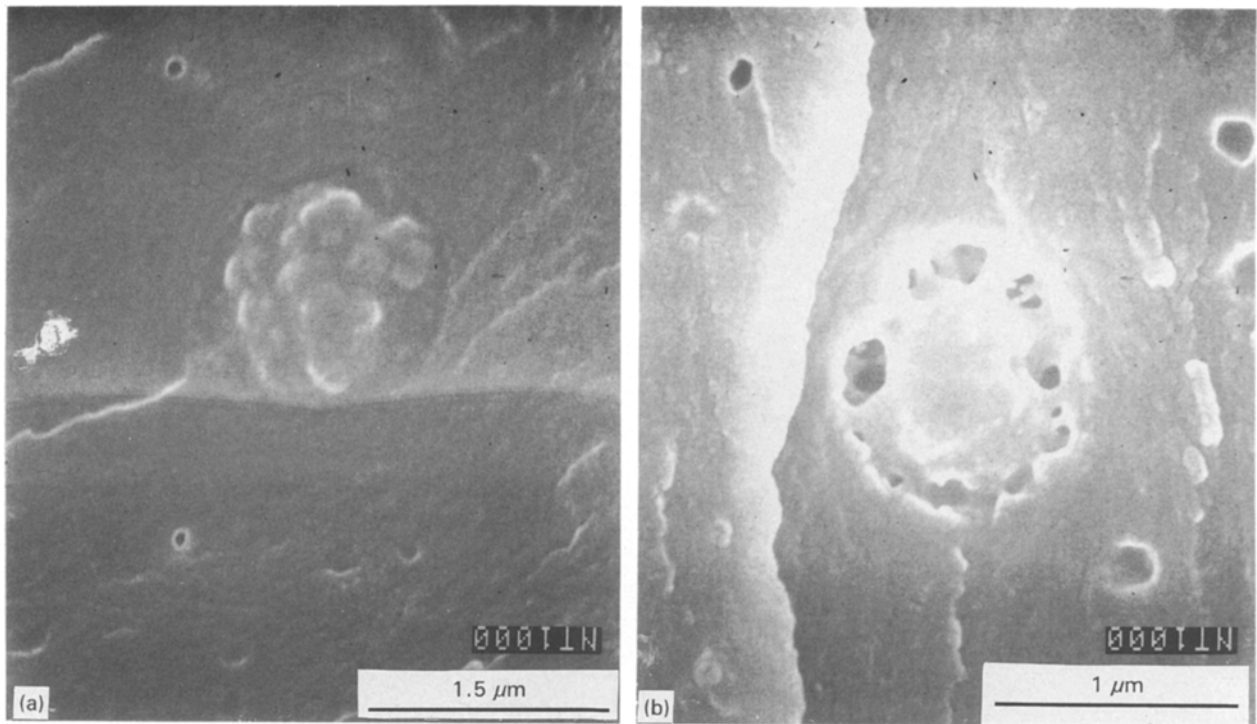


Figure 8 SEM micrographs of fracture surfaces of 10 p.h.r. ITPU-modified UPE based on PTMG 1000: (a) fractured in liquid nitrogen, (b) fractured at room temperature.

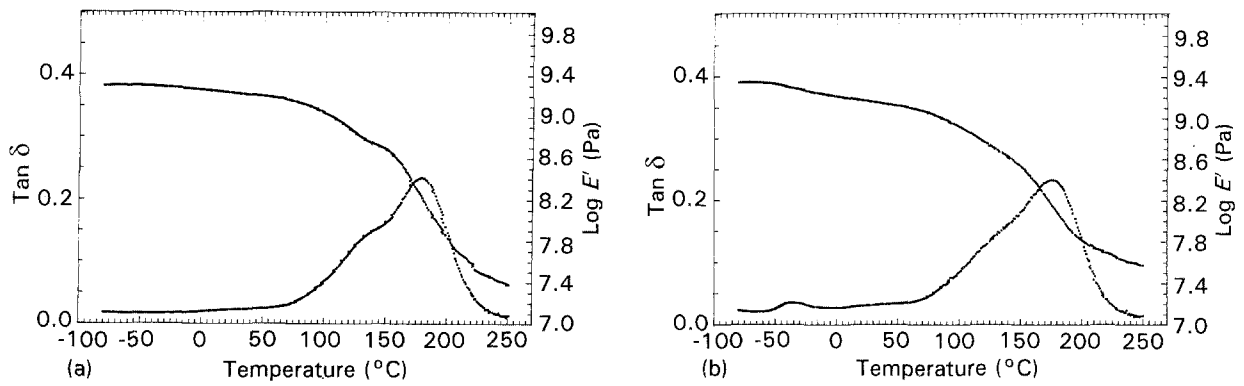


Figure 9 Dynamic mechanical spectra: (a) neat UPE, (b) PPG 2000-based ITPU-modified UPE.

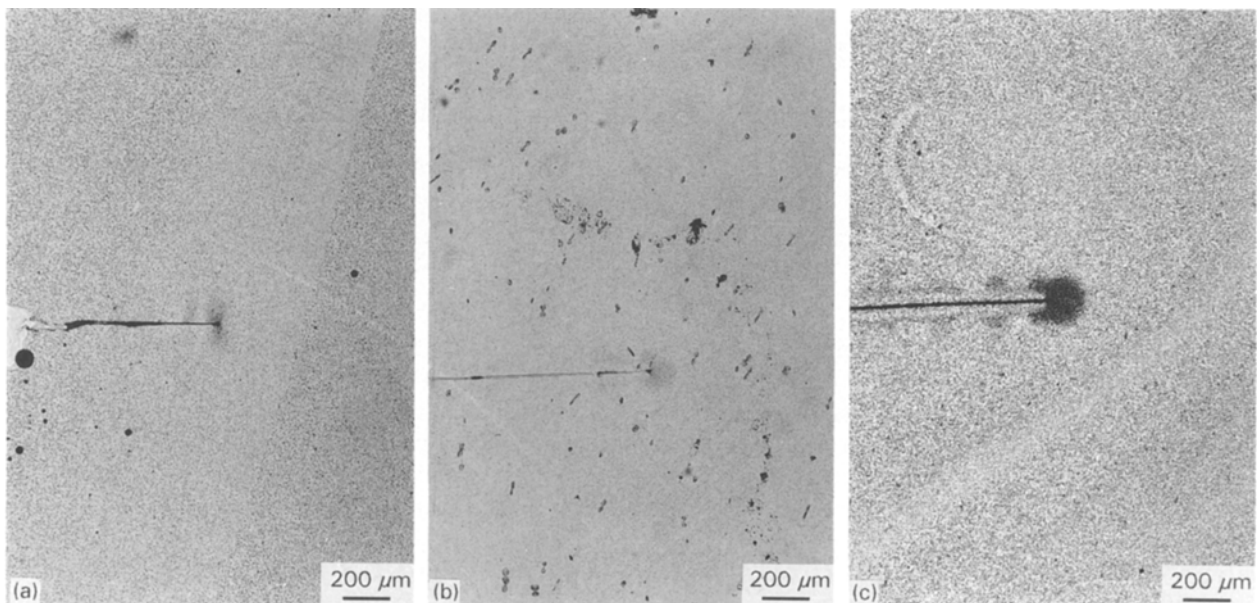


Figure 10 Optical micrographs of thin section taken mid-plane and near the crack tip of DN-4PB sample of 10 p.h.r. HTPU-modified UPE, based on (a) PTMG 650, (b) PTMG 1000, (c) PTMG 2000.

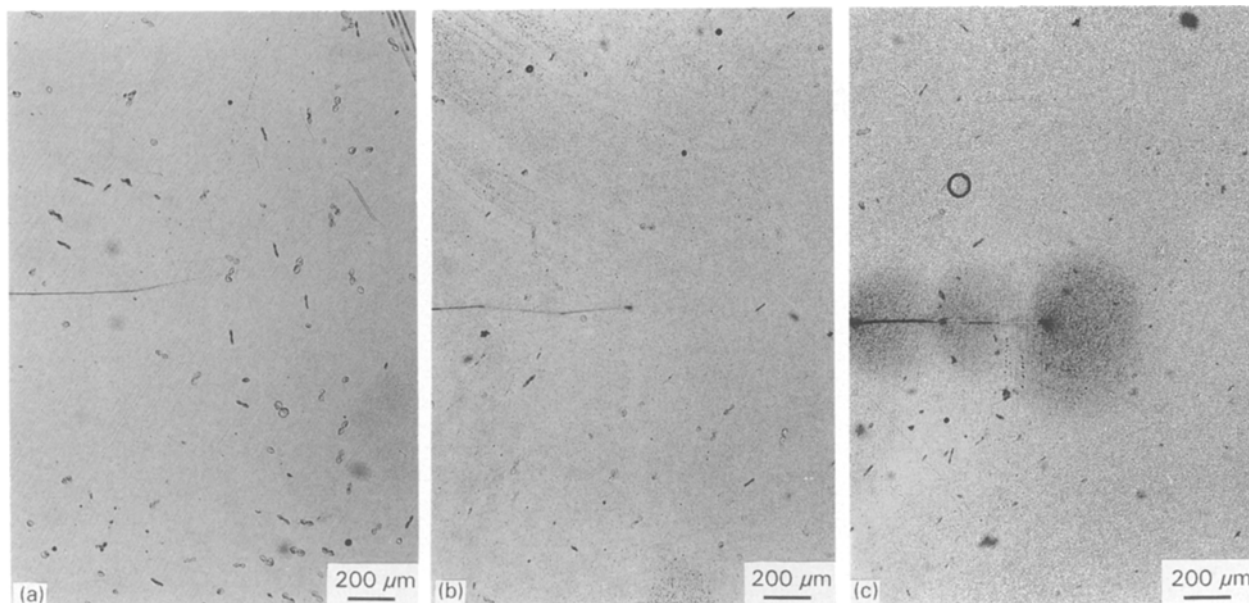


Figure 11 Optical micrographs of thin section taken mid-plane and near the crack tip of DN-4PB sample of 10 p.h.r. ITPU-modified UPE, based on (a) PTMG 650, (b) PTMG 1000, (c) PTMG 2000.

in order for a particle to cavitate it must be embedded in a hydrostatic stress field, otherwise it cannot cavitate. The size of hydrostatic stress field is equivalent to the 'formal plastic zone' proposed by Irwin [12]. Irwin's formal plastic zone size may be estimated, for the plain strain case, by

$$r_p = (1/6\pi)(K_{IC}/\sigma_y)^2$$

where  $r_p$  is the radius of the plastic zone,  $K_{IC}$  is the critical stress intensity factor, and  $\sigma_y$  is the yield stress.

Irwin's formal plastic zone size of UPE calculated using  $K_{IC} = 0.49 \text{ MPa m}^{1/2}$  and  $\sigma_y = 91 \text{ MPa}$  is  $1.54 \text{ }\mu\text{m}$ , which is too small to be a critical particle size for bridging. Our experimental observations reveal that the critical particle size for bridging is approximately  $5 \text{ }\mu\text{m}$ . Even though the average particle size of PPG 4000-based PU rubber-modified UPE is around  $3 \text{ }\mu\text{m}$ , most of the particles are larger than  $5 \text{ }\mu\text{m}$  due to the bimodal distribution of particle size, as shown in Figs 4d and 6d. Therefore the major toughening mechanism of PPG 4000-based PU rubber modified-UPE is rubber bridging, instead of debonding and cavitation.

When the thin sections of tested tensile specimens were examined by cross-polarized light to confirm the existence of shear bands, shear bands could not be detected in all samples. As Pearson & Yee [11] could not observe shear band formation for a highly cross-linked epoxy, shear band formation seems to be impossible without modification of the main chain in rubber toughening of UPE.

#### 4. Conclusions

The toughening mechanism of PU rubber-modified UPE was investigated by SEM and optical microscopy. The energy dissipating mechanisms varied de-

pending on the adhesion strength between rubber particle and matrix and particle size of rubber. The toughening mechanisms were debonding in HTPU-modified UPE, cavitation in ITPU-modified UPE, and rubber particle bridging with large particle-size rubber.

However shear bands, which are a major energy dissipating mechanism with rubber-modified epoxies, are not observed with any rubber-modified UPE. It seems that shear bands cannot be formed as UPE is a highly cross-linked thermoset with very short chain length between cross-links. Thus toughness enhancement is very limited and much smaller than that of the rubber-modified epoxy.

In the rubber toughening of UPE, cavitation in the rubber particles seem to be more effective than debonding or particle bridging, and chemical bonding between rubber particles and matrix is a prerequisite for cavitation. In the present experiments, a 1.9 times increase in fracture toughness of UPE was achieved with the formation of cavitated particles, whereas there was a 1.5 times increase with the formation of debonded particles. Thus in order to maximize the fracture toughness of rubber-modified UPE, more cavitated particles and high cavitation resistance are required. This means the particle size of rubber should be small and the properties of rubber should be controlled to have suitable cavitation resistance. In the real systems, as the particle size, the volume fraction, and the properties of rubber are varied simultaneously, it is difficult to differentiate the quantitative contribution of each parameter. Conclusively, the toughness of highly cross-linked thermosets can be maximized without the sacrifice of cross-link density by incorporating well-bonded small particles with balancing the particle size, the volume fraction, and the properties of rubber.

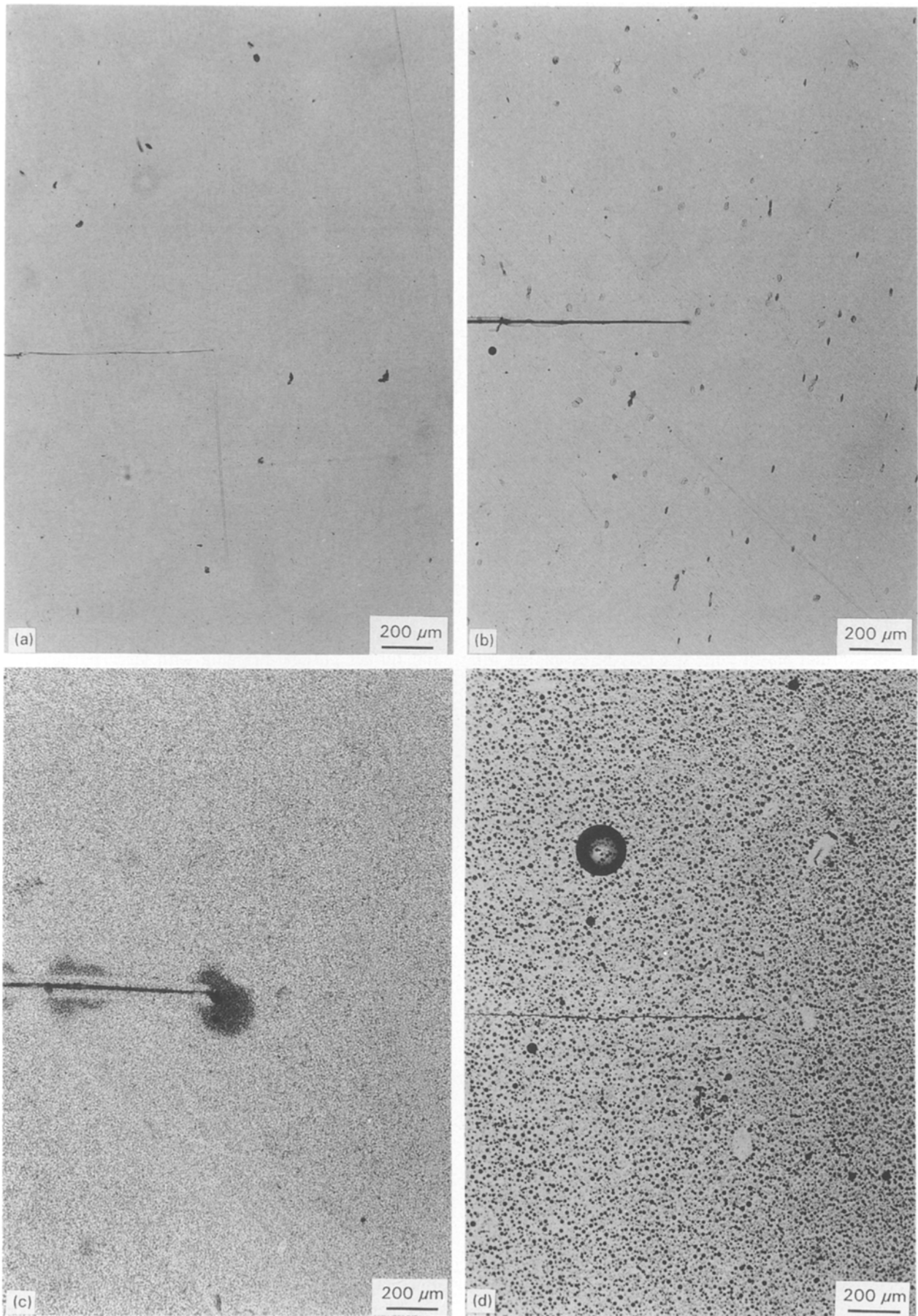


Figure 12 Optical micrographs of thin section taken mid-plane and near the crack tip of DN-4PB sample of 10 p.h.r. HTPU-modified UPE, based on (a) PPG 750, (b) PPG 1000, (c) PPG 2000, (d) PPG 4000.

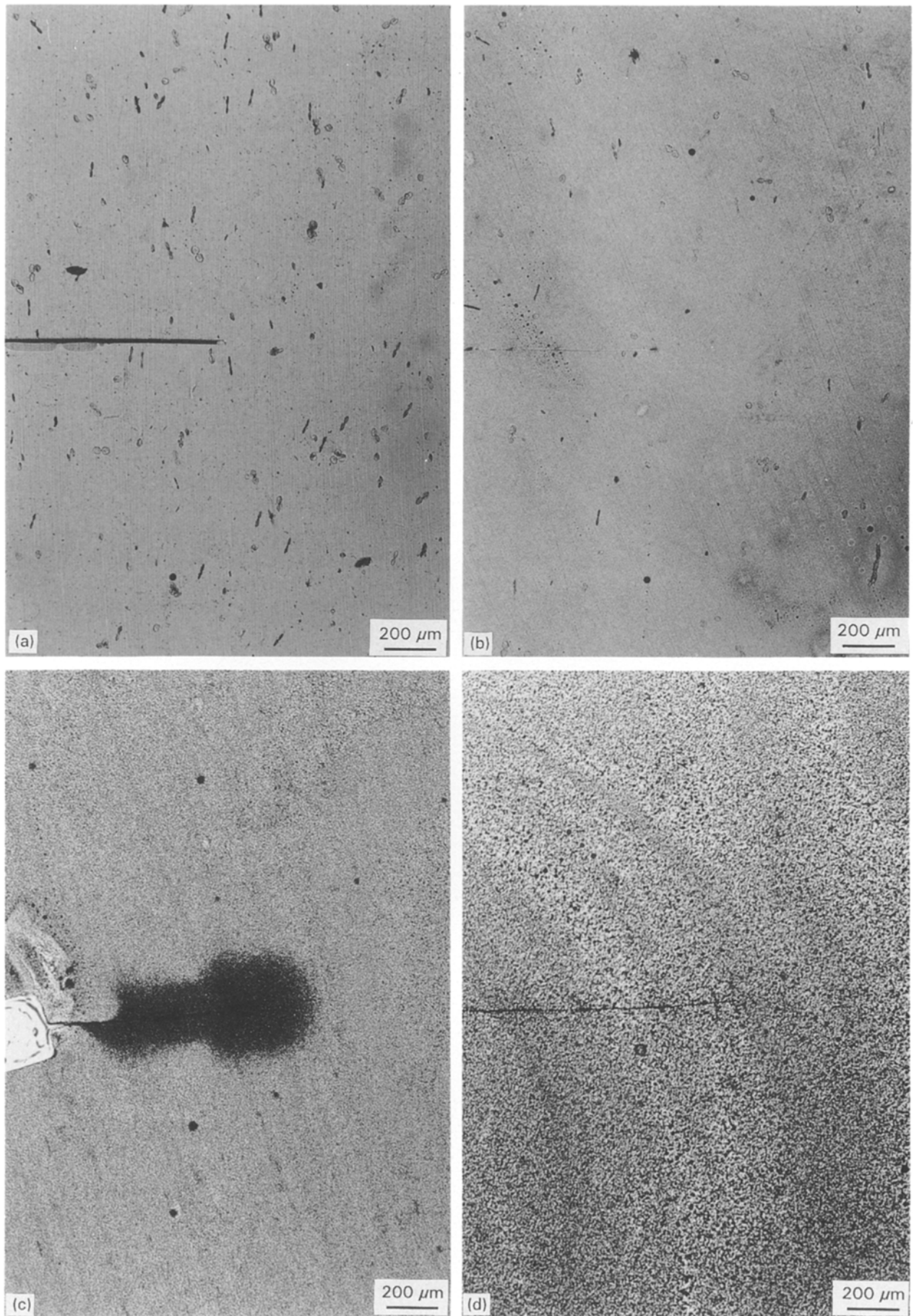


Figure 13 Optical micrographs of thin section taken mid-plane and near the crack tip of DN-4PB sample of 10 p.h.r. ITPU-modified UPE, based on (a) PPG 750, (b) PPG 1000, (c) PPG 2000, (d) PPG 4000.

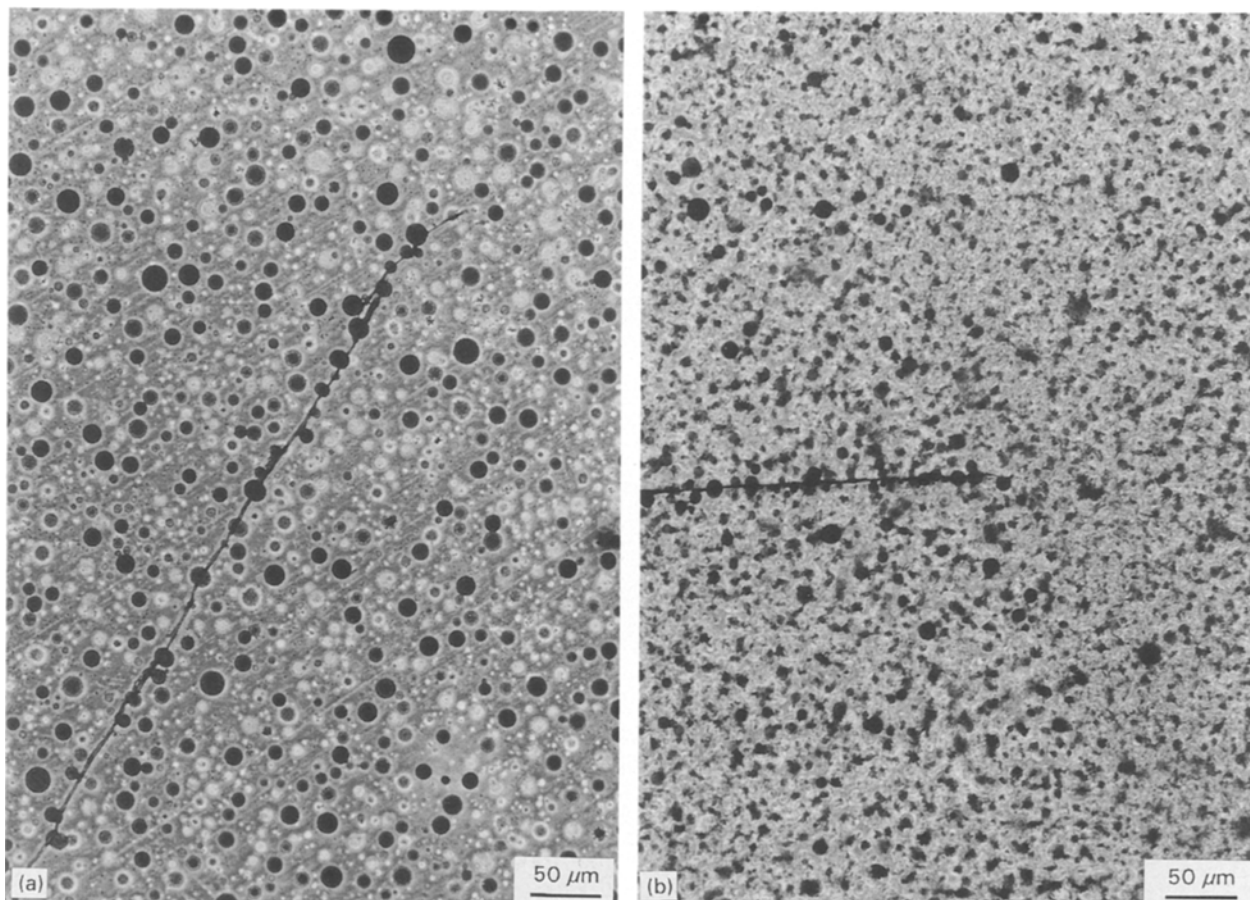


Figure 14 Optical micrographs of thin section taken mid-plane and near the crack tip of DN-4PB sample of PPG 4000 based PU-modified UPE, (a) HTPU, (b) ITPU.

## Acknowledgement

This paper was supported by the Research Institute of Industrial Science and Technology.

## References

1. J. N. SULTAN and F. J. MCGARRY, *Polym. Eng. Sci.* **13** (1973) 29.
2. E. J. KRAMER, in "Advances in Polymer Science", edited by H. H. Kaush, Vol. 52/53 (Springer-Verlag, Berlin, 1983) ch. 1.
3. Y. HUANG and A. J. KINLOCH, *J. Mater. Sci.* **27** (1992) 2753.
4. *Idem, ibid.* **27** (1992) 2763.
5. A. J. KINLOCH, S. J. SHOW, D. A. TOD and D. L. HUNSTON, *Polymer* **24** (1983) 1341.
6. R. A. PEARSON and A. F. YEE, *J. Mater. Sci.* **21** (1986) 2475.
7. Y. HUANG and A. J. KINLOCH, *Polymer* **33** (1992) 1330.
8. *Idem, J. Mater. Sci. Lett.* **11** (1992) 484.
9. S. C. KUNZ-DOUGLASS, P. W. R. BEAUMONT and M. F. ASHBY, *J. Mater. Sci.* **15** (1980) 1109.
10. R. A. PEARSON and A. F. YEE, *ibid.* **24** (1989) 2571.
11. *Idem, ibid.* **26** (1991) 3828.
12. G. R. IRWIN, *Appl. Mater. Res.* **3** (1964) 65.
13. P. D. TETLOW, J. F. MANDELL and F. J. MCGARRY, in Proceedings of 34th Annual Technical Conference, Reinforced Plastics/Composites Institute (Society of the Plastics Industry, Inc, New York, 1979) section 23F.
14. G. A. CROSBIE and M. G. PHILLIPS, *J. Mater. Sci.* **20** (1985) 182.
15. *Idem, ibid.* **20** (1985) 563.
16. S. N. TONG and P. T. K. WU, *Polym. Plast. Eng.* **27** (1988) 519.
17. D. S. KIM, K. CHO, J. H. AN and C. E. PARK, *J. Mater. Sci. Lett.* **11** (1992) 1197.
18. H. J. SUE, R. A. PEARSON, D. S. PARKER, J. HUANG and A. F. YEE, *Polym. Preprints* **30** (1988) 147.
19. T. KANAZAWA, S. MACHIDA, S. MOMOTO and Y. HAGIWARA, in Proceedings of the 2nd International Conference on Fracture, Brighton, April 1969, edited by P. L. Pratt (Chapman & Hall, London, 1969) p. 1.
20. H. J. SUE, *Polym. Eng. Sci.* **31** (1991) 270.
21. A. S. HOLIK, R. P. KAMBOUR, S. Y. HOBBS and D. G. FINK, *Microstruct. Sci.* **7** (1979) 35.
22. S. WU, *Polymer* **26** (1985) 1855.

Received 30 March  
and accepted 8 October 1993